Journal of Nuclear Materials 385 (2009) 552–558

Contents lists available at ScienceDirect

Journal of Nuclear Materials

journal homepage: www.elsevier.com/locate/jnucmat

Study of the temperature evolution of defect agglomerates in neutron irradiated molybdenum single crystals

O.A. Lambri [a,b,*], G.I. Zelada-Lambri [b], G.J. Cuello [c,e], P.B. Bozzano [d], J.A. García [e]

[a] Instituto de Física Rosario. Member of the CONICET's Research Staff, Avda. Pellegrini 250, (2000) Rosario, Santa Fe, Argentina
[b] Facultad de Ciencias Exactas, Ingeniería y Agrimensura, Universidad Nacional de Rosario, Laboratorio de Materiales, Escuela de Ingeniería Eléctrica, Avda. Pellegrini 250, (2000) Rosario, Santa Fe, Argentina
[c] Institut Laue Langevin, 6, rue Jules Horowitz, BP 156, 38042 Grenoble, France
[d] Laboratorio de Microscopía Electrónica. Unidad de Actividad Materiales, Centro Atómico Constituyentes, Comisión Nacional de Energía Atómica, Avda. Gral. Paz 1499, (1650) San Martín, Argentina
[e] Departamento de Física Aplicada II, Facultad de Ciencias y Tecnología, Universidad del País Vasco, Apdo. 644, 48080 Bilbao, País Vasco, Spain

ARTICLE INFO

Article history:
Received 23 November 2008
Accepted 31 December 2008

PACS:
61.50.–f
61.72–y
61.12–q
61.16–d
72.15.Eb

ABSTRACT

Small angle neutron scattering as a function of temperature, differential thermal analysis, electrical resistivity and transmission electron microscopy studies have been performed in low rate neutron irradiated single crystalline molybdenum, at room temperature, for checking the evolution of the defects agglomerates in the temperature interval between room temperature and 1200 K. The onset of vacancies mobility was found to happen in temperatures within the stage III of recovery. At around 550 K, the agglomerates of vacancies achieve the largest size, as determined from the Guinier approximation for spherical particles. In addition, the decrease of the vacancy concentration together with the dissolution of the agglomerates at temperatures higher than around 920 K was observed, which produce the release of internal stresses in the structure.

1. Introduction

Nuclear materials are exposed to external stresses and at the same time to irradiation and temperature. Because of that, it is of great importance to understand the behaviour of the defects produced as a function of temperature, in order to predict the long time behaviour of these materials.

Molybdenum has a high melting point, a high specific heat, good corrosion, creep resistance and strength at high temperatures. In addition, it has a relatively low thermal neutron cross-section. These qualities make molybdenum attractive for the use in the nuclear industry [1,2].

Several works have been reported about the radiation damage in molybdenum [3–13]. The appearance of five stages of recovery has been proposed depending of their temperature range. They can be defined as stage I, below 120 K; stage II, from 120 K to 330–350 K; stage III, from 330–350 K to 600 K; stage IV, from 600 K to 850–900 K and stage V, for temperatures higher than 850–900 K [3,8,10,14]. For instance, in stage III, it has been reported that in neutron irradiated molybdenum at room temperature, a subsequent annealing at temperatures between 473 K and 573 K lead to an increase in the yield stress and in the ultimate tensile strength (UTS); which is promoted by the movement of vacancies [8,10,14]. Besides this, in mechanical spectroscopy tests, it was found that annealing at temperatures of the stage V is required for restoring the characteristic of the damping peak related to the dragging of jogs by the dislocation under movement assisted by vacancy diffusion [15]. Indeed, the damping peak in neutron irradiated samples is less intense and appears at smaller temperatures (600 K) than in only pre-strained samples (800 K). Subsequent annealing during the mechanical spectroscopy tests at 973 K did not change too much the peak position of the relaxation in irradiated samples. However, an annealing at 1073 K moves the peak position to around 800 K, due to the recovery of the structure in stage V [15,16].

It should be pointed out that, in the above referenced works both, the movement and the interaction of vacancies and/or clusters of vacancies with dislocations have been observed indirectly, through the study of the response of several experimental techniques. For this reason, we have realised small angle neutron scattering (SANS) studies in order to corroborate more directly the evolution of the vacancies and/or aggregates as a function of

* Corresponding author. Address: Laboratorio de Materiales, Escuela de Ingeniería Eléctrica, Facultad de Ciencias Exactas, Ingeniería y Agrimensura, Universidad Nacional de Rosario, IFIR-CONICET, Avda. Pellegrini 250, (2000) Rosario, Santa Fe, Argentina. Tel.: +54 341 4802649/4802650x125; fax: +54 341 4821772/4802654.
E-mail address: olambri@fceia.unr.edu.ar (O.A. Lambri).

0022-3115/$ - see front matter © 2009 Elsevier B.V. All rights reserved.
doi:10.1016/j.jnucmat.2008.12.312

temperature and then to confirm the previous obtained results. In addition, scarce information is reported concerning to the shape and/or concentration of the interacting defects with dislocations as a function of the annealing temperature.

In the present work we have performed 'in situ' SANS as a function of temperature, differential thermal analysis, electrical resistivity and transmission electron microscopy studies in neutron irradiated single crystalline molybdenum, for checking the evolution of defects agglomerates promoted by the neutron irradiation in the temperature interval between room temperature (RT) and 1200 K.

The use of SANS for observing the evolution of defects agglomerates promoted by the neutron irradiation is particularly interesting in molybdenum, due to the fact that the traditional technique of positron annihilation spectroscopy for watching the vacancies and/or clusters of vacancies cannot be used. This is because the very high background due to the emitted radiation of the neutron irradiated samples. In addition, when molybdenum is irradiated with low flux and low dose, SANS appears to be an excellent complement to transmission electron microscopy (TEM) characterisation, especially when the TEM resolution is not enough to resolve agglomerates of few vacancies.

2. Experimental

Single crystals used in this work were prepared from zone refined single-crystal rods of molybdenum in A.E.R.E., Harwell. The residual resistivity of the samples is about 8000, tungsten being the main residual impurity. Samples with the ⟨1 1 0⟩ crystallographic tensile axis were annealed and then deformed in extension (3%) at a constant speed of 0.03 cm/min, followed by torsion (1%) at RT. After the plastic deformation process the samples were irradiated, at RT, with neutrons during 10 h. Neutron irradiation was performed at the Siemens SUR 100 nuclear reactor, RA-4, of the National University of Rosario – National Atomic Energy Commission of Argentina. The fluxes of thermal, epithermal and fast neutrons at the position where the samples were placed, were 5.7×10^{11} n/m^2 s, 8.1×10^{9} n/m^2 s and 5.0×10^{11} n/m^2 s, respectively. Taking into account previous reported works [13,17] an estimation of the irradiation dose in dpa (displacement per atom) is around 10^{-5}. In addition, an estimation of the amount of vacancies promoted in the samples during 10 h irradiation, calculated by means of SRIM2006.02 [18] would be around 5×10^{14}, which gives rise to an initial (after irradiation) vacancy concentration of about 5 ppm. Details about the sample characteristics and irradiation conditions are described elsewhere [15].

The electrical resistivity, ER, measurements were performed at room temperature by the eddy current decay technique [19]. The ER values were measured both prior to irradiation and after irradiation as a function of the annealing temperature. Samples used in ER were single crystalline cylindrical rods of 5 mm diameter and 50 mm length. Annealing treatments were performed by heating the sample at a rate of 1 K/min under pure argon at normal pressure followed by cooling into the furnace, under the same protective atmosphere.

Differential thermal analysis, DTA, studies were performed in a Setaram TGA-92 equipment using platinum–rhodium crucibles. The heating and cooling runs were performed with a rate of 5 K/min, under argon atmosphere at normal pressure. Samples in DTA studies were cylinders of 5 mm diameter and 2 mm length, which were taken from the same rod of the sample used in ER studies.

For transmission electron microscopy (TEM) examinations, thin foils were prepared with the double jet technique using 12% H_2SO_4 in methyl alcohol. Observations were carried out in a Phillips CM200 transmission electron microscope, operated at 200 kV.

Small angle neutron scattering (SANS) studies were performed at the D11 instrument (Institute Laue-Langevin) as a function of temperature from RT up to different maximum temperatures, using a heating rate of about 4 K/min, under high vacuum. Cooling runs were also recorded. Data collected on the two-dimensional detector were azimuthally averaged, corrected for background and absorption and normalised to the absolute cross-section, employing GRASP V. 3.4 software [20–22]. The two dimensional detector was located at 5.5 m, using a counting time of 90 s. The incident neutron wavelength was 0.45 nm, giving rise to momentum transfer values between 0.2 nm^{-1} and 1.3 nm^{-1}. The sample used in SANS experiments was a cylinder of 2 mm length and 5 mm diameter, which was cut from the same rod of the sample used in the ER test. The axis of the cylinder (⟨1 1 0⟩) was positioned parallel to the incident beam into a vanadium sample holder. The sample was subjected to the following thermal history 'in situ' at the diffractometer: first heating up to 1200 K, subsequent cooling down to 400 K. New heating up to 1270 K followed by an annealing at this temperature (1270 K) during 1 h and subsequent cooling down to room temperature.

3. Results and discussion

3.1. Electrical resistivity and differential thermal analysis studies

The behaviour of the electrical resistivity of irradiated samples is shown in Fig. 1, in the left axis. Empty symbol indicates the value of the ER before the neutron irradiation. The ER increases, as the annealing temperature is increased, up to a maximum at around 600 K. At higher temperatures the ER curve begins to decrease. In addition, a stage (plateau) around 1000 K appears and subsequently at higher temperatures the ER starts to decrease again. As it was recently explained [15], the increase in the ER values from 300 K up to 600 K, coincides with the stage III of recovery in irradiated samples; which was related to the movement of vacancies [8,10,14]. It has been reported that in neutron irradiated molybdenum at room temperature, a subsequent annealing at temperatures between 473 K and 573 K produces an increase in the yield stress and in the ultimate tensile strength (UTS) [8], due to the appearance of internal stresses within the temperature range of the stage III [15]. The appearance of internal stresses in stage III, due to the reorganization of the defects out

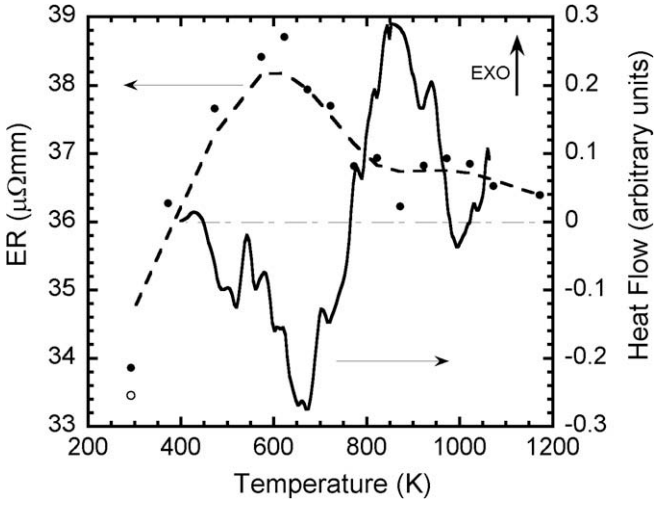

Fig. 1. Left axis: behaviour of the electrical resistivity at room temperature as a function of the annealing temperature, full points. Empty point, ER value prior to irradiation. Right axis: heat flow as a function of temperature measured from differential thermal analysis in an irradiated sample.

of thermodynamic equilibrium, leads to the locking of dislocations during the first run-up in temperature for irradiated samples in the mechanical spectroscopy test. It gave rise to an amplitude dependent damping background without the appearance of the damping peak (at around 800 K). In contrast, by increasing the annealing temperature to 973 K (stage V), which is higher than the temperature for the maximum observed in the ER curves, the damping peak appears during the cooling without dependence on the amplitude of vibration. This behaviour was explained considering the movement of vacancies to the dislocations [15,23,24]. Besides this, it was also reported that the yield stress and the UTS also decreases with an increase of the annealing temperature at temperatures higher than about 973 K [8,16].

Also in the right axis in Fig. 1 is shown the thermogram measured for an irradiated sample, after the subtraction of the base line. DTA spectrum exhibits a clear endothermic reaction within the 450–750 K temperature range, with a maximum at around 650 K followed by an exothermic reaction developed between around 750 K and 1000 K, with a maximum at about 820 K. It should be mentioned that it was complicated to detect these heat flow changes, from DTA measurements. Even if they were reproducible in different tests, the magnitude of the reactions was quite small. It could be related with the small quantity of defect promoted by the low flux irradiation, see Ref. [15].

The temperature intervals where these reactions appear are in reasonable agreement with the salient features of the ER curve. The first endothermic peak at around 650 K can be related to the maximum in ER which corresponds to the stage III of recovery. In fact, the development of internal stresses in the Stage III can be thermodynamically related to the increase of internal energy from a metastable state after irradiation to another metastable state at a higher energy valley, when vacancies start their movement.

The exothermic reaction can be related to the decrease in the ER values from 600 K and with the development of the stages IV and V of recovery. In these stages the movement of vacancies towards the dislocations would take place in order to decrease the free energy of the structure. Indeed, it is in agreement with the appearance of the damping peak in the mechanical spectroscopy tests during the cooling, after an annealing to 973 K (stage V) [15,23]. At temperatures higher than 1000 K, the DTA curve seems to develop another exothermic reaction related to a further recovery of the irradiated structure at higher temperatures [10,14,15]. A further recovery of the radiation damage at temperatures higher than 1223 K has been also reported earlier in the literature [14–16].

As it was already remarked in Section 1, the movement of vacancies above described and reported in previous works, is proposed on the basis of indirect results obtained from several experimental techniques. For this reason, we have made SANS studies in order to corroborate more directly the evolution of the vacancies and/or aggregates as a function of temperature and then to confirm the previous obtained results.

3.2. The SANS diagrams

Figs. 2–4 show the differential scattering cross-section, I, as a function of q (q being the modulus of the scattering vector), measured in situ at the D11 diffractometer for different temperatures, in the previously neutron irradiated sample. For the sake of clarity, only some curves of the whole set of the experimental data are plotted in the figures. Curves shown in the plots are those corresponding to temperatures where clear changes appear in the I vs. q behaviour of the sample, as a way to highlight their differences. Indeed, they were studied mainly for q smaller than about 0.4 nm^{-1}, which is where the differences can be observed more easily. The error in each experimental point in the plotted figures is less than 5%.

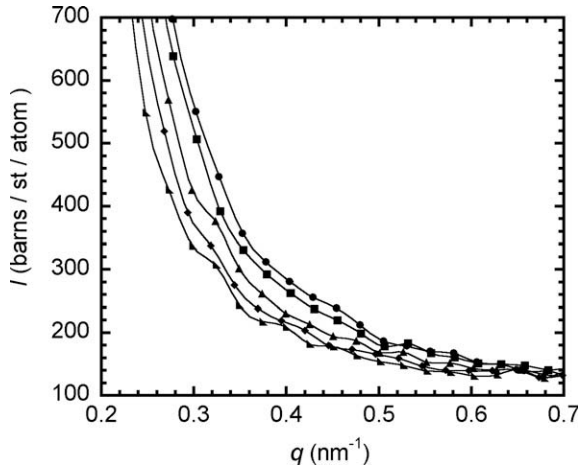

Fig. 2. Scattering intensity as a function of the scattering vector q for different temperatures measured during the first heating. Circles: 296 K, squares: 608 K, triangles: 919 K, diamonds: 1035 K, squared triangles: 1203 K.

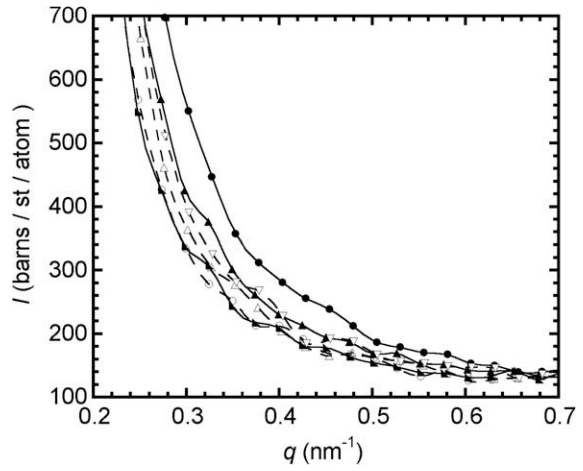

Fig. 3. Scattering intensity as a function of the scattering vector q for different temperatures measured during the first cooling, empty symbols: circles: 1175 K, triangles: 954 K, inverted triangles: 754 K. Full symbols, values measured during the first heating: circles: 296 K, triangles: 919 K, squared triangles: 1203 K.

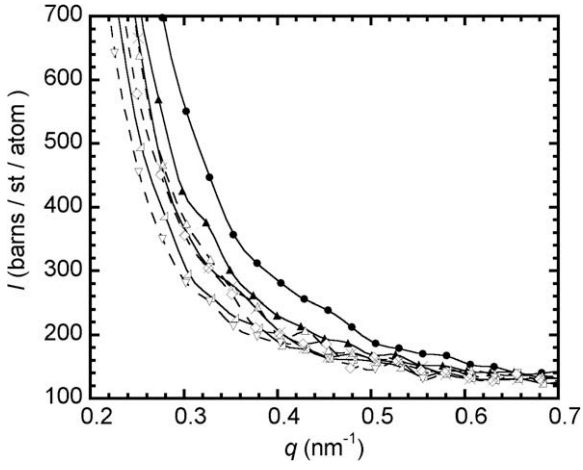

Fig. 4. Scattering intensity as a function of the scattering vector for different temperatures measured during the thermal cycles. First heating, full symbols: circles: 296 K, triangles: 919 K. First cooling, x: 954 K. Second heating, empty symbols: triangles: 922 K, squared triangles: 1264 K. Measurement at 1196 K after annealing at 1270 K–1 h: inverted empty triangles. Second cooling, empty diamond: 945 K.

Fig. 2 shows the behaviour of I for different temperatures measured during the first heating up to 1200 K. The curve measured at room temperature (296 K), prior to starting the warming run, exhibits an increase in I for small values of q. This increase is the strongest one in comparison to the reported for the other curves, owing to the generation of defects and/or defect-clusters promoted by the neutron irradiation. In the curve corresponding to 608 K, a slow decrease in the intensity, for q smaller than 0.5 nm^{-1} can be observed. The curves which were measured at intermediate temperatures between 296 K and 608 K, did not exhibit clear changes between them.

The first decrease at 608 K in the scattering curves, measured during the first warming, can be related to a smaller quantity of defects interacting with the incident beam, owing to that some of them during their movement were annihilated in some sinks of the lattice. However, not all the vacancies that moved at this temperature were annihilated. Indeed, a reorganisation of vacancies is also occurring, as it is revealed thorough the maximum measured in ER and to the endothermic reaction in the DTA thermogram (see Fig. 1). This reorganisation of defects produces the pinning of the dislocations which lead to the increase both in the yield stress [8] and the UTS [8,14] and to the damping background without the appearance of the damping peak during the first heating after irradiation in the mechanical spectroscopy tests [15].

A subsequent decrease in the values of I could be found for the curve measured at 919 K, for q values smaller than about 0.5 nm^{-1}. As it can be inferred from Fig. 2, this decrease is larger, with respect to the curve recorded at 296 K, than the previous one occurred at 600 K. It indicates that the quantity of defects promoted by the irradiation is decreased by the recovery within the temperatures of the stage V, in agreement with the decrease in the values of ER after its maximum and with the exothermic reaction in the thermogram of Fig. 1. This reduction in the I values within the stage V of recovery can be related to the migration of vacancies towards the dislocations, owing to the appearance after annealing to 973 K of the damping peak [15]. The next decrease in the values of the intensity of scattering appears for temperatures higher than 1050 K and it is related in part to a subsequent recovery of the structure and also to a temperature effect of the lattice. Regarding to the recovery mechanism, this decrease results in agreement with (a) the start of the new decrease in the ER curve for temperatures at around 1050 K, (b) the beginning of the exothermal reaction at around 1050 K in the DTA test and (c) the restoration of the damping peak-temperature in irradiated samples during mechanical spectroscopy tests after annealing to about 1050 K. Indeed, the temperature of the damping peak after irradiation was around 600 K and it is restored to the values exhibited in a sample only plastically deformed without irradiation, i.e., 800 K, when the temperature of annealing during the mechanical spectroscopy tests is increased at around 1050 K [15].

It should be stressed that, the recovery effects observed in SANS studies up to annealing temperatures of about 1050 K, are related to the recovery of vacancy-type point defects out of thermodynamic equilibrium, since the dislocation structure is still stable, i.e., the dislocation density and arrangement of dislocations is the same. In fact, it can be assured since both, the peak height of the damping peak does not change in strained samples during successive thermal cycles up to temperatures smaller than 1050 K [23]; and from TEM studies that reveal the same kind of dislocation arrangement and dislocation density [15,16].

Fig. 3 shows the behaviour of I vs. q curves for temperatures where clear changes appear during the cooling (empty symbols), after the first heating up to 1200 K (showed in Fig. 2). In order to facilitate the comparison of the results, curves measured during the first heating at 296 K, 919 K and 1203 K were also plotted by means of full symbols.

The I values measured in all curves during the cooling are smaller than the corresponding ones of the curve measured during the first heating at 919 K. In fact, the curve measured at 754 K during the cooling (inverted empty triangles) is similar to the measured at 919 K during the first heating (full triangles). Nevertheless, it is observed that the I curves after having reaching the smallest value at 1203 K during the heating, increase during the cooling. These values are slightly smaller than the measured during the first heating at approximately the same temperature, as it can be inferred by comparing the curves of empty and full triangles. Therefore, the decrease in the scattering curves measured at temperatures higher than 1050 K could have also overlapped to the recovery effect, the effect of the temperature increase on the lattice during the warming, as it was previously mentioned. In contrast, the decrease measured at around 920 K is controlled mainly by the recovery of the structure in stage V, involving the movement of vacancies to dislocations.

Fig. 4 shows a summary of the I vs. q curves measured at different temperatures during all warming and cooling runs measured in SANS experiments. Full circles and triangles correspond to curves measured during the first heating at 296 K and 919 K, respectively. The curve indicated by x corresponds to a measurement at 954 K during the first cooling. Empty equilateral triangles and empty squared triangles correspond to measured data during the second warming at 922 K and 1264 K, respectively. The inverted empty triangles correspond to a temperature of 1196 K measured during the second cooling after the annealing at 1270 K during 1 h. The curve measured at 1270 K at the end of the annealing treatment, when the cooling has started (not plotted in the figure), overlaps to the curve measured at 1196 K. Empty diamonds correspond to a curve measured at 945 K during the second cooling after the annealing treatment. As it can be seen from Fig. 4, the annealing at 1270 K leads to smaller I vs. q curves than before annealing. The measured curve at 1196 K during the second cooling (inverted empty triangles) is even smaller than the one measured at 1264 K during the second warming (empty left squared triangles). In addition, the curve measured at 945 K during the second cooling (empty diamonds) is clearly smaller than another curves measured at very close temperatures, during the previous two warming and cooling.

The behaviour of the whole group of I vs. q curves for heating and cooling runs during the SANS experiment corroborates that at around 608 K, the excess of vacancies promoted by the irradiation start their movement, where some of them are annihilated at the sinks of the lattice, in agreement with previous works [8,15,16]. In addition, at around 920 K the recovery of the structure in the stage V of recovery starts. At around 920 K the structure of the molybdenum moves from an energy valley towards a smaller energy valley, in agreement with the results of Fig. 1 and previously reported results [15]. The decrease in the I vs. q curves is related to the decrease in the quantity of vacancies out of thermodynamic equilibrium, due to their movement to dislocations as it was above already mentioned.

The behaviour of the scattering curves at higher temperatures, is in accordance with a temperature of recovery of the radiation damage higher than 1223 K, as it was mentioned [10,14,15] and with both, the decrease in the ER curve at temperatures of about 1200 K and the starting of another exothermic reaction at around 1100 K in the DTA thermogram. At higher temperatures than around 1050 K both, the quantity of vacancies and the dislocation density decreases by recovery [15,23].

As summary of this section we have corroborated that: (a) at 600 K a reorganisation of the structure take place where the concentration of vacancies decreases, but there exist still a lot of them out of thermodynamic equilibrium. (b) at temperatures higher than 920 K (stage V, $T > 850$–900 K), the concentration of vacancies out of thermodynamic equilibrium decreases markedly.

On the other hand, in order to show the powerful resolution of SANS for this kind of characterisation, a TEM micrograph is shown in Fig. 5, where the small agglomerates promoted in these low flux neutron irradiated samples were not resolved.

3.3. The Guinier plots

In order to study the evolution of the arrangement of vacancies in irradiated samples during the annealing treatments, Guinier plots ($\ln I$ vs. q^2) [20,22,25] for the scattering curves measured during the SANS tests, were performed. The Guinier approximation for the cross-section is [20]:

$$I = \frac{d\sigma}{d\Omega} = C_G \exp\left(-\frac{q^2 R_g^2}{3}\right), \quad (1)$$

where C_G is the Guinier constant and R_g is the radius of gyration of a particle. Assuming a spherical particle of radius, R, we have:

$$R_g = \frac{3}{5}R. \quad (2)$$

Then, from the slope in a $\ln I$ vs. q^2 plot, the radius of the particle, assumed spherical can be obtained.

Fig. 6(a) shows the Guinier plots for scattering curves measured during the first warming in the SANS experiment. In this figure the base line is shifted for clarity. As it can be seen from a naked-eye examination, curves for temperatures smaller than 816 K exhibit a Guinier zone (linear region) between about 0.1 nm^{-2} and 0.3 nm^{-2}. Nevertheless, in order to diminish ambiguous analysis, straight lines were fitted by means of Chi-square (χ^2) fit [25]. The behaviour of the Chi-square coefficient was evaluated for different groups of ($\ln(I)$ vs. q^2) data pairs beginning from about 0.7 nm^{-2} towards the higher ones. Data pairs ($\ln(I)$ vs. q^2) were added and subtracted in order to sweep the q^{-2} range between 0.7 nm^{-2} and 0.04 nm^{-2}. In addition, the q^2 interval for performing the best fitting was also obtained from the same procedure, as it was already reported [25]. Fitted straight lines are plotted by means of full lines in Fig. 6(b). The length of the interval for fitting is indicated in the figure by means of the length of the straight line. In Fig. 6(b) are only plotted the straight lines for the so called low q^2 range, with Chi-square coefficients smaller than 2×10^{-3}, where the linearity is completely evident. Details of the fitted curves are listed in Table 1.

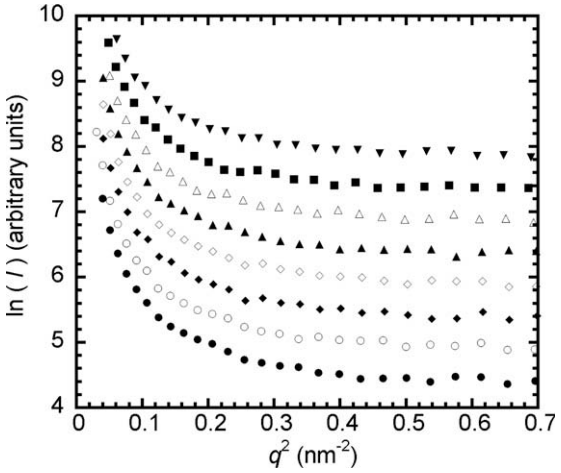

Fig. 6a. Guinier representation for an irradiated sample measured during the first heating for different temperatures: full circle: 296 K, empty circle: 393 K, full diamond: 546 K, empty diamond: 608 K, full triangle: 745 K, empty triangle: 816 K, full square: 877 K, inverted full triangle: 988 K.

Straight lines for the so called high q^2 range were not plotted, since the slope of the curves exhibited a markedly dispersion, even if the Chi-square coefficients were still smaller than for the low q^2 range, see Table 1. In addition, straight lines at q^2 values smaller than about 0.1 nm^{-2} cannot involve more than tree points ($\Delta q^2 \sim 3 \times 10^{-2}$ nm^{-2}) and consequently they were not taken into account in the present work.

The appearance of straight lines also in the zone of high q^2 values, even if the behaviour of their slopes did not revealed physical meaning, can be related to the non-spherical shape of the agglomerates of vacancies [20]. Therefore, the behaviour of the radius of the particles as a function of temperature, calculated by combining Eqs. (1) and (2) from the slope of the straight lines in the low q^2

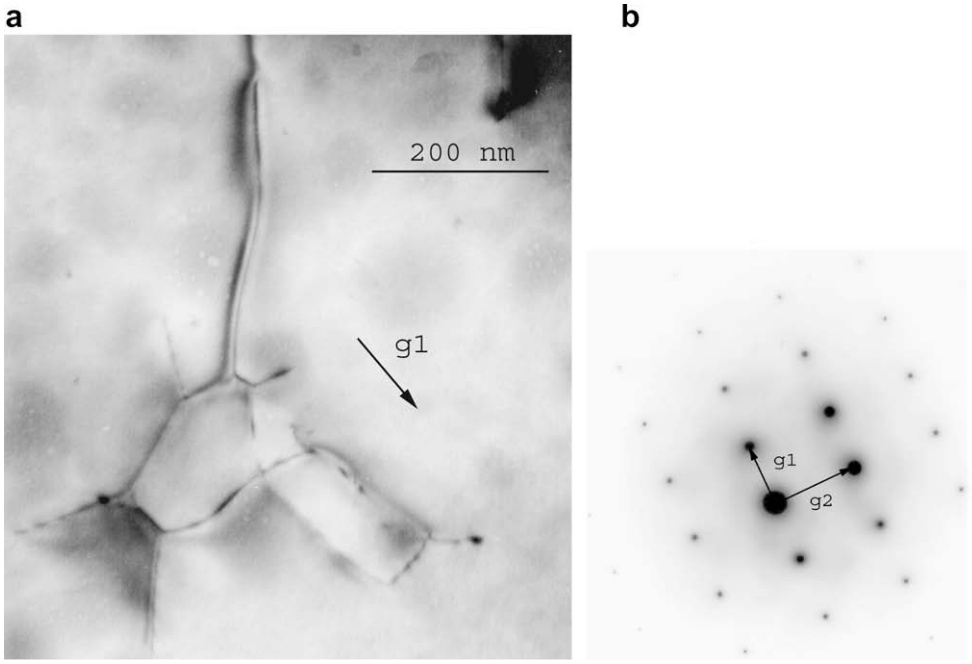

Fig. 5. (a) TEM micrograph for an irradiated sample. (b) Selected area diffraction pattern: g1 = (−1, 0, 1), g2 = (0,−2, 0), zone axis [1, 0, 1].

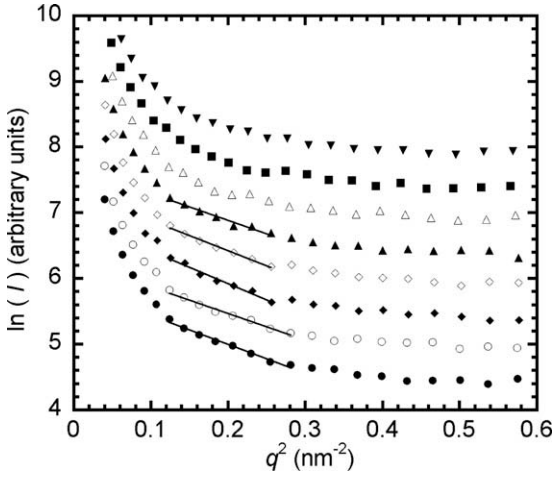

Fig. 6b. Straight lines fitted to the Guinier representation, according to fitted parameters detailed in Table 1. See explanation in the text. Symbols correspond as in Fig. 6(a).

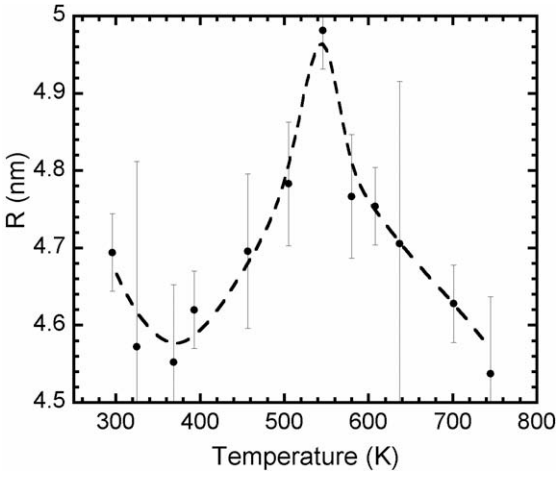

Fig. 7. Size of the particles considered as spheres as a function of temperatures, calculated from the Guinier approximation. See explanation in the text.

Table 1
Details of the fitting procedure for the low and high q^2 ranges in the Guinier plots. Subscripts 0 and f mean, the initial and the final value for q^2 range, respectively, where the fitting procedure was done. m and h are the slope (arb. units nm^2) and the ordinate (arb. units) of the fitted straight lines, respectively.

T (K)	q^2 range	$q_0^2 \times 10/q_f^2 \times 10$ (nm^{-2})	Fitted points	m	h	$\chi^2 \times 10^3$
296	Low	1.2459/2.8123	8	−440.65	5.879	1.08
	High	2.5500/4.3160	7	−160.57	5.138	0.21
393	Low	1.2448/2.8106	8	−408.00	6.286	1.03
	High	3.1082/4.6812	6	−70.551	5.280	0.11
540	Low	1.2561/2.5646	7	−496.31	6.917	1.15
	High	2.8276/4.3350	6	−138.21	6.049	0.63
608	Low	1.2533/2.5606	7	−458.44	7.342	0.498
	High	2.5606/4.6695	8	−123.00	6.508	0.71
745	Low	1.2517/2.5587	7	−411.68	7.711	1.47
	High	2.5587/4.0008	6	−172.00	7.107	0.52
816	Low	1.2342/2.7948	8	−367.70	8.089	3.58
	High	2.5334/4.9842	9	−104.20	7.403	0.82
877	Low	1.2021/2.4871	7	−524.10	8.842	3.45
	High	2.4871/4.5702	8	−127.44	7.949	1.27
919	Low	1.2177/2.5096	7	−424.81	9.164	2.00
	High	2.5096/4.6009	8	−111.81	8.401	0.74

range, is an approximation and it must be considered as a qualitative observation of the evolution of the defects in the microstructure as a function of temperature. Fig. 7, shows the behaviour of the radius of the particles (assumed to be spheres) as a function of temperature.

It should be highlighted that at temperatures of about 550 K, the largest size of agglomerates is obtained, in reasonable agreement with the ER and DTA results. In addition, the increase in the yield stress and UTS [8] and the appearance of an amplitude dependent damping background without the damping peak during the first heating after irradiation [15] are also in agreement with the decrease in the mobility of dislocations by the development of agglomerates of vacancies promoted by the irradiation within the stage III. Increasing the temperature at values higher than those for the maximum in the ER curve (approx. 600 K), the size of agglomerates of vacancies decreases (Fig. 7), allowing the movement of dislocation to start which leads to the subsequent decrease in internal stresses of the microstructure.

At temperatures higher than 816 K which are in stage IV and also close to temperatures within the stage V of recovery, the non-appearance of Guinier zones can be related to both, the dissolution of aggregates controlled thermally, and to the absorption of vacancies by the dislocations, as it was previously proposed [15]. In addition, during the second heating run Guinier zones were not found for the temperatures detailed in Table 1 within the studied q^2 interval, owing to which vacancy agglomerates do not appear.

As summary of this section, in stage III (300–350 K to 600 K) the movement of defects out of thermodynamic equilibrium take place, leading to the growing of agglomerates, which give rise to the reported behaviour in the electrical resistivity, DTA, mechanical spectroscopy, yield stress and UTS studies. At higher temperatures than about 816 K the dissolution of agglomerates starts.

4. Conclusions

The behaviour of the scattering curves as a function of temperature was appropriate for detecting the mobility of defects and their rearrangement and/or dissolution in stages III, IV and V in neutron irradiated molybdenum at low flux and dose. This result represents a valuable tool for studying the evolution of the vacancies in irradiated molybdenum, particularly when consider positron annihilation and transmission electron microscopy limitations.

The starting of the mobility of vacancies out of thermodynamic equilibrium at temperatures within the stage III of recovery was found. At around 550 K, the agglomerates of vacancies achieve the largest size, as determined from the Guinier approximation for spherical particles. In addition, within the stage III a small decrease of the vacancy concentration was observed.

It was verified that the decrease of the vacancy concentration and also the dissolution of agglomerates occur at temperatures of the stage V, leading to the release of internal stresses.

Acknowledgements

The Institut Laue – Langevin (ILL), D11 Instrument (Grenoble, France), is acknowledge for the allocated neutron beamtime (Exp. No.: 1-01-38). We acknowledge also to Professor J.N. Lomer for the interest in the present work and for the single crystal samples. This work was partially supported by the Collaboration Agreement between the Universidad del País Vasco and the Universidad Nacional de Rosario Res. CS.788/88 – 1792/2003, UPV224.310-14553/02, Res. 3469/2007 and the new one signed Res. pending 2008, the CONICET-PIP No. 5665 and the PID-UNR (ING 115) 2005–2007 and (ING 227) 2008–2009. O.A.L. wishes to acknowledge to Rev. P. Ignacio Peries for the support with the health.

References

[1] D.J. Mazey, C.A. English, J. Less Common Met. 100 (1984) 385.
[2] S. Nemat-Nasser, W. Guo, M. Liu, Scr. Mater. 40 (1999) 859.
[3] B. Mastel, L. Brimhall, Acta Metall. 13 (1965) 1109.
[4] L. Brimhall, B. Mastel, T.K. Bierlein, Acta Metall. 16 (1968) 781.
[5] R.C. Rau, J. Moteff, R.L. Ladd, J. Nucl. Mater. 40 (1971) 233.
[6] C.C. Matthai, D.J. Bacon, J. Nucl. Mater. 125 (1984) 138.
[7] J. Cornelis, P. de Meester, L. Stals, J. Nihoul, Phys. Stat. Sol. (a) 18 (1973) 515.
[8] A.S. Wrosnsky, A.A. Johnson, Philos. Mag. 213 (1963) 1067.
[9] H.B. Afman, Phys. Stat. Sol. (a) 13 (1972) 623.
[10] J. Nihoul, Symp. on Radiation Damage in Solids and Reactor Materials, vol. I, IAEA, Vienna, 1962, SM 25.
[11] G.L. Kulcinski, H.E. Kissinger, Phys. Stat. Sol. (a) 2 (1970) 267.
[12] A.A. Johnson, J. Less Common Met. 2 (1960) 241.
[13] B.V. Cockeram, J.L. Hollenbeck, L.L. Snead, J. Nucl. Mater. 324 (2004) 77.
[14] B.V. Cockeram, J.L. Hollenbeck, L.L. Snead, J. Nucl. Mater. 336 (2005) 299.
[15] G.I. Zelada-Lambri, O.A. Lambri, P.B. Bozzano, J.A. García, C.A. Celauro, J. Nucl. Mater. 380 (2008) 111.
[16] G.I. Zelada-Lambri, PhD thesis, Rosario National University, Rosario, Argentina, 2008.
[17] T.S. Byun, M. Li, B.V. Cockeram, L.L. Snead, J. Nucl. Mater. 376 (2008) 240.
[18] J.F. Ziegler, J.P. Biersack, U. Littmark, The Stopping and Range of Ions in Solids, Pergamon, New York, 1985.
[19] J.A. García, S. Hull, S. Messoloras, R.J. Stewart, J. Phys. E. Sci. Instrum. 21 (1987) 466.
[20] R.J. Stewart, in: A.V. Chadwick, M. Terenzi (Eds.), NATO ASI Series, Plenun, New York, 1985, p. 95.
[21] C. Dewhurst, GRASP (Graphical Reduction and Analysis SANS) User Manual V. 3.40, Institut Laue langevin, Grenoble, France, April 2003.
[22] G. Kostorz, in: R.W. Cahn, P. Haasen (Eds.), Physical Metallurgy, 3rd Ed., North Holland Physics Publishing, Amsterdam, 1983, p. 793.
[23] G.I. Zelada-Lambri, O.A. Lambri, J.A. García, J. Nucl. Mater. 353 (2006) 127.
[24] C.L. Matteo, O.A. Lambri, G.I. Zelada-Lambri, P.A. Sorichetti, J.A. García, J. Nucl. Mater. 377 (2008) 370.
[25] O.A. Lambri, G.J. Cuello, W. Riehemann, J. Lucioni, Int. J. Mat. Res. (formerly Z. Metallkunde.) 98 (2007) 501.